

Wireless Tracking of Cranial Bone Regeneration via Biodegradable Implant Degradation Monitoring

Mahdi Salimitorkamani*, Burak Ferhat Ozcan*, and Sema Dumanli*

*Electrical and Electronics Engineering Dept., Bogazici University, Istanbul, Turkiye, sema.dumanli@bogazici.edu.tr

Abstract—Advances in additive manufacturing and biomaterials are ushering in a new era of cranial implants, where patient-specific 3D-printed biodegradable devices are becoming standard practice. Here, a partially conformal slot antenna is proposed to monitor the regeneration process of cranial bone with a biodegradable cranial implant. The on-body antenna operates at 2.4 GHz and is constructed using a substrate of Rogers 3010 and a flexible superstrate of graphite doped silicone. A biodegradable lattice-shaped implant with a radius of 12 mm is embedded within the cranial region and covered with a liquid layer to emulate realistic post-surgical conditions. By varying the implant radius from 12 mm to 2 mm, the bone regeneration and implant degradation is simulated. The resonant frequency of the on-body antenna changes as the defect heals due to the change in effective permittivity of the implanted region. It has been shown that a 2 mm change in radius results in at least 53 MHz change. This shift confirms the antenna’s high sensitivity to bone regeneration progression and its potential for real-time, non-invasive monitoring of cranial healing.

I. INTRODUCTION

Cranial implants are medical devices designed to repair skull defects resulting from trauma, surgical procedures, or congenital conditions [1]. Typically fabricated from biocompatible materials, such as titanium, medical-grade polymers, or biodegradable composites, these implants restore structural integrity while providing critical protection to the brain. Recent advances have focused on biodegradable materials that actively promote bone regeneration, such as polylactic acid (PLA), polyglycolic acid (PGA), and poly-D,L-lactic acid (PDLLA), thereby eliminating the need for permanent foreign implants [2]. In addition, it is now feasible to 3D print biodegradable implants tailored to the specific anatomical site and the individual patient [3].

Monitoring the cranial healing process is crucial for tracking the recovery period following implantation [4]. Conventional modalities for monitoring post-implant healing—CT, MRI, and tracer-based bone scans—provide high resolution but involve high costs, ionizing radiation exposure (for CT), and lengthy workflows [5]–[7]. These limitations have increased interest in complementary approaches, such as microwave-based monitoring, which offers a non-ionizing, cost-effective and widely deployable alternative for tracking bone regeneration and implant degradation [8]–[11]. Such innovations aim to improve patient outcomes by enabling personalized post-surgical care and reducing complications.

Current research demonstrates several innovative methodologies for monitoring bone regeneration with unique application. These include the use of biosensors to track critical

parameters such as infection, pH, and temperature during bone regeneration [12]. Other methods involve the use of magnetoelasticity-based (MB) sensors to monitor the in vitro degradation of polylactic acid (PLA) artificial bone (PAB), a promising implant material for bone defect repair [13]. Additionally, AI-based monitoring systems have demonstrated effectiveness in evaluating bone healing progression [14]. In a complementary approach, recent research has comprehensively summarized advancements in osteoporosis detection and fracture diagnosis (including forearm, femur, tibia, and femoral fractures) through reflection and transmission coefficient analysis [15]. For cranial applications specifically, in [16], one-dimensional pulsed radar techniques with resistively loaded antennas were shown to effectively monitor skull healing by observing changes in the amplitude of the matched filter responses. In a related study [17], short-pulse radar techniques were applied to cranial surgery phantom models, demonstrating the ability to detect skull defects. Ultra-wideband (UWB) sensors based on resistively loaded dipole antennas were also developed for use with cranial surgery phantoms [18]. Reference [4] demonstrates the variation in resonance frequency for monitoring bone healing progression from post-surgery to complete recovery in newborns, showing a frequency shift of approximately 60 MHz between pre-operative measurements and one-year post-operative follow-up. In [19], the design of an open-ended circular waveguide (OECW) antenna was proposed for pediatric craniosynostosis patients. This device was optimized for non-invasive skull healing monitoring, with emphasis on frequency tuning and material selection to enhance sensitivity across different healing stages. Microwave-based monitoring uses the contrast between the permittivity of healing bone, soft tissue, and biodegradable implants. The resonant frequency of an antenna shifts as the permittivity in its near-field changes. Hence if the regeneration occurs in the near-field of an antenna, the antenna can be used as a sensor. Although recent studies have demonstrated the feasibility of this approach for continuous monitoring of the healing process [17], challenges remain in optimizing sensitivity for early-stage healing detection, achieving scalable real-time monitoring, and modeling realistic implant degeneration scenarios.

In this study, we propose a partially conformal on-body slot antenna resonating at 2.4 GHz for real-time, non-invasive monitoring of biodegradation of cranial implants. The antenna is designed with a flexible graphite doped silicone superstrate that allows the antenna to partially conform to the human

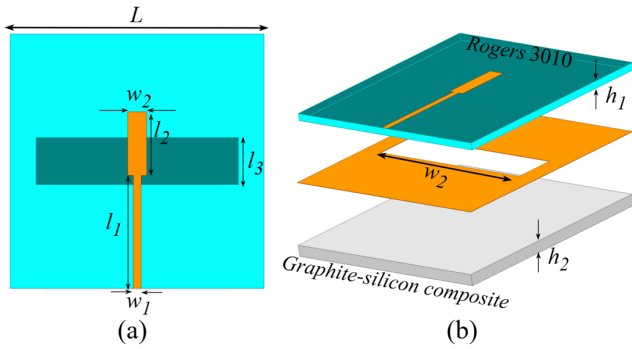


Fig. 1. (a) Top-view of the proposed slot antenna, (b) exploded view of the Layers configuration: Rogers 3010 (top layer), copper, and flexible graphite-silicon composite base (bottom layer). Design parameters (all in mm) are given as: $L = 40$, $w_1 = 1.8$, $w_2 = 3$, $l_1 = 15$, $l_2 = 10$, $l_3 = 8$, $h_1 = 1.27$, $h_2 = 2$.

head. This material provides both mechanical flexibility for anatomical conformity and improves the impedance-matching to the head hence the in-body propagation. The layer has a relative permittivity of 12.4 and a loss tangent of 0.036 at 2.4 GHz. The high permittivity decreases the reflection from air to skin boundary as well as decreasing the near-field losses. This dual functionality of mechanical robustness and dielectric matching sets the proposed antenna apart. Measurable resonance frequency shifts exceed 570 MHz during bone regeneration. To the best of the authors' knowledge, this is the first study in the literature to monitor cranial bone regeneration by tracking the biodegradation of a realistic biodegradable lattice implant.

The remainder of this paper is organized as follows. Section II details the design of the on-body slot antenna. Section III presents the model of the biodegradable implant. Section IV analyzes the biodegradation monitoring and corresponding results. Finally, Section V provides the concluding remarks.

II. THE ON-BODY SLOT ANTENNA MODEL

Fig. 1 presents the proposed slot antenna design for wireless monitoring of cranial bone regeneration. The slot antenna is sandwiched between a superstrate and a substrate. It is fed with a microstrip line. The substrate is Rogers 3010 ($\epsilon_r = 10.2$, $\tan \delta = 0.002$) while the superstrate is developed from flexible graphite-silicone composite ($\epsilon_r \approx 12.4$, $\tan \delta = 0.036$). The superstrate ensures conformal contact with cranial curvatures while providing impedance matching to biological tissues. A magnetic antenna is chosen here since magnetic fields couple inductively and are less susceptible to attenuation from the conductive properties of biological tissues compared to electric fields, which couple capacitively and cause immediate charge buildup and significant energy loss at the surface. This characteristic enables a more efficient deeper sensing capability for monitoring the cranial implant degradation. The complete design parameters are provided in Fig. 1.

III. THE BIODEGRADABLE IMPLANT MODEL

The biodegradable implant is 3D printed in a lattice structure with a radius of 12 mm. The lattice structure mimics

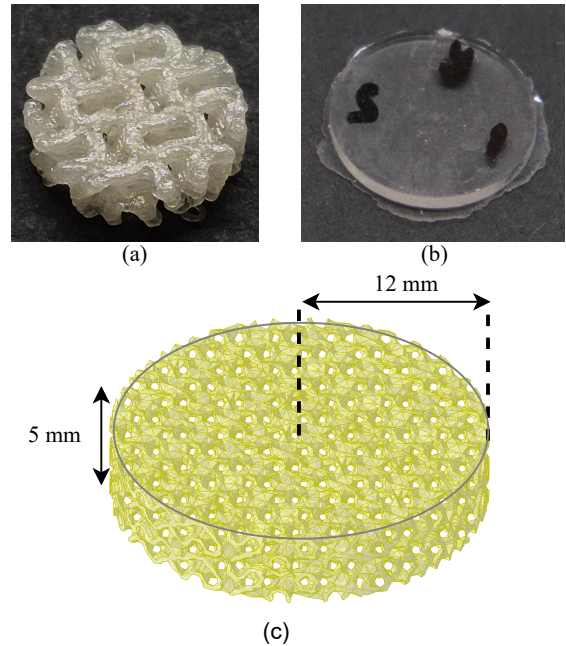


Fig. 2. (a) Lattice structure of the cranial implant fabricated using PLGA-824S, (b) solid PLGA sample prepared for dielectric characterization, and (c) dimensions and simulation model of the implant.

bone mechanics and promotes ingrowth and vascularization [20]. A patient specific design can be generated in the shape of the matching bone that matches the mechanical properties required [20]. Here, the cranial implant with a lattice structure, as shown in Fig. 2(a), is printed using PLGA-824S (LG 824 S, Poly (L-lactide-co-glycolide)). The dielectric characterization of PLGA is performed using a solid sample fabricated via the mini injection molding technique, as seen in Fig. 2(b), and measured with the Speag DAK 3.5. It has a relative permittivity of $\epsilon_r = 2.5$ and a loss tangent of $\tan \delta = 0.015$ at 2.4 GHz. The simulation model of the implant and its geometry are given in Fig. 2(c).

IV. WIRELESS MONITORING OF BIODEGRADATION

The monitoring system comprising the on-body slot antenna with a realistic head phantom containing the embedded lattice-shaped biodegradable implant is shown in Fig. 3 (a) and (b). The implant is merged in a liquid layer ($\epsilon_r \approx 70$) to model post-surgical conditions. The combination of the low-permittivity implant surrounding with the high-permittivity liquid results in an effective relative permittivity of approximately 35 at the operating frequency for the implant region. The surrounding cranial bone tissue has a relative permittivity of $\epsilon_r = 11.4$ at 2.4 GHz. The difference between these permittivity values serves as the primary mechanism for the resonance shift during the monitoring process.

The relationship between the radius of the biodegradable implant and the on-body slot antenna's resonance frequency is given in Fig. 4 reflecting progressive bone regeneration. As the implant radius decreases from fresh post-surgical condition of 12 mm to almost healed value of 2 mm, the resonance

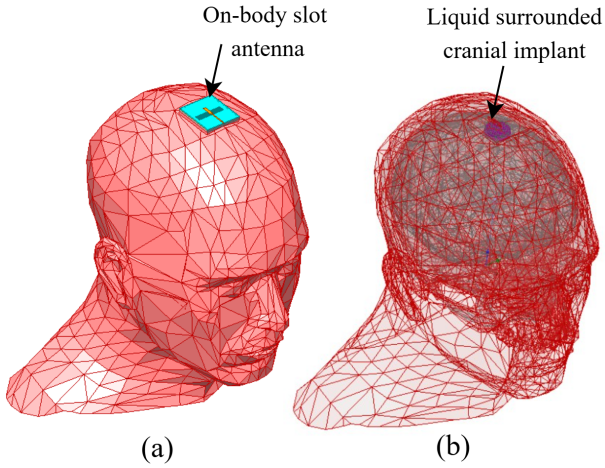


Fig. 3. (a) Head phantom model assembly with on-body slot antenna, (b) implant placement within the phantom.

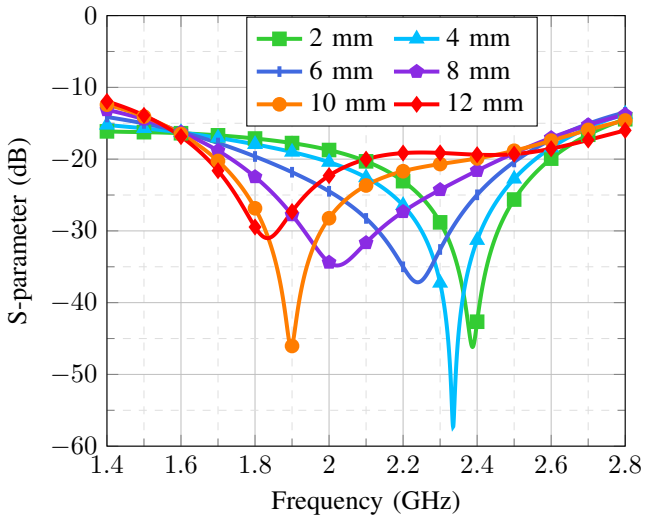


Fig. 4. Resonance frequency shifts versus implant degradation state (S-parameters showing 570 MHz downward shift (2.4 GHz to 1.83 GHz) as implant radius decreases from 12 mm (fresh cavity) 2 mm (healed bone).

frequency increases from approximately 1.83 GHz to 2.4 GHz—a total shift of over 570 MHz. This trend results from the decreasing effective permittivity of the implant region.

It is important to note that, the shifts from radius of 4 mm to 2 mm is only 53 MHz indicating reduced dielectric loading as bone regeneration progresses. This trend can be attributed to the shrinking interaction volume with lower permittivity materials during the healing process. The simulations validate the system's sensitivity to bone regeneration stages, where frequency shifts serve as quantitative markers for:

- **Early healing** (implant radius: 12–8 mm): $\Delta f \approx 190$ MHz
- **Intermediate mineralization** (implant radius: 8–4 mm): $\Delta f \approx 330$ MHz

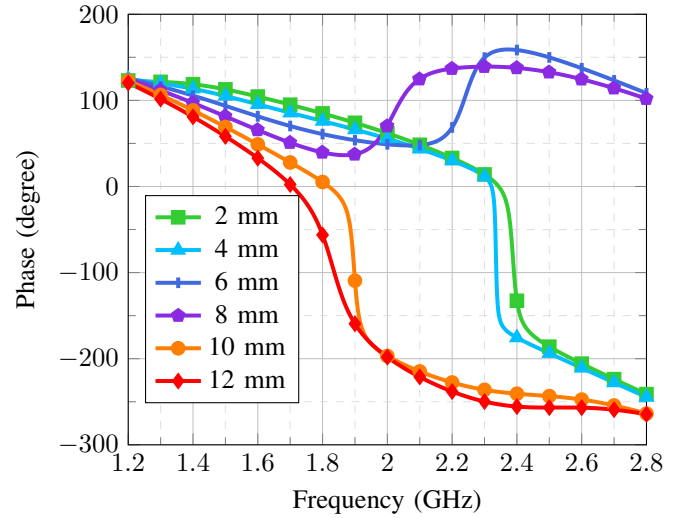


Fig. 5. Phase response of the slot antenna across varying implant radii (2–12 mm) at 2.4 GHz.

- **Late-stage healing** (implant radius: 4–2 mm): $\Delta f \approx 53$ MHz

The consistent frequency response across all healing stages demonstrates strong clinical potential for monitoring degradation rates of biodegradable implants, with approximately 50 MHz/mm sensitivity throughout the regeneration process.

The phase response in Fig. 5 reveals detectable phase variations at the operational frequency of 2.4 GHz as the implant radius changes, providing complementary information to the magnitude-based S_{11} analysis. At 2.4 GHz, the phase exhibits a progressive shift of approximately 55 degrees as the implant radius decreases from 12 mm to 2 mm, corresponding to the bone regeneration process. This phase change results from alterations in the electromagnetic wave propagation delay through the implant region, where the effective electrical length varies with the changing dielectric properties. The higher permittivity of the fluid-filled cavity at larger implant radii introduces greater phase delay compared to the lower permittivity of healed bone tissue. The consistent, monotonic phase shift across different implant radii demonstrates the potential for phase-based monitoring as an additional sensing modality.

Fig. 6 (a) and (b) compare the electric field distribution at 2.4 GHz for cranial regions with and without the biodegradable implant, respectively. The presence of the implant significantly alters the field penetration and energy distribution within the cranial tissues. When the implant is present, the high-permittivity fluid-filled cavity creates a stronger dielectric contrast at the tissue-implant interface, leading to enhanced field concentration around the implant region and modified wave propagation through the multi-layer structure due to lensing. Conversely, the absence of the implant results in a more uniform field distribution through the homogeneous bone tissue, with reduced field perturbation and smoother energy penetration into deeper cranial layers. This distinct

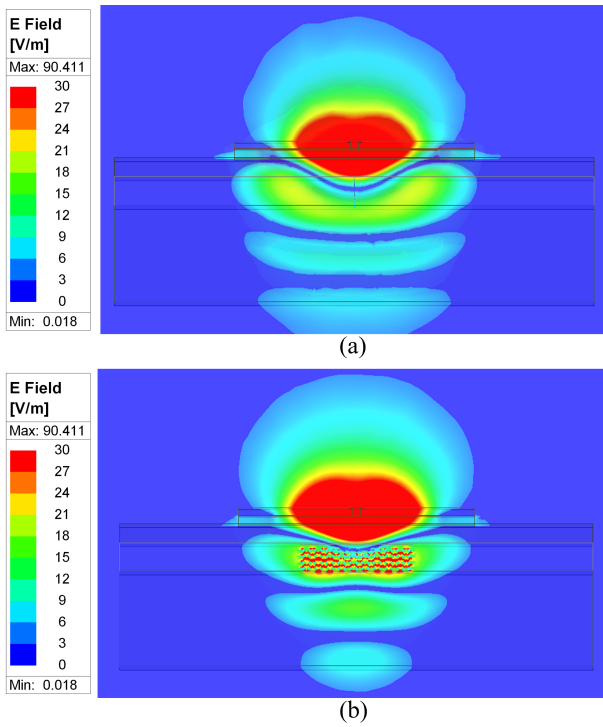


Fig. 6. E-field radiation within the head model, (a) without implant, and (b) with lattice-shaped implant.

field behavior demonstrates the implant's role as a dielectric perturbation source that modifies the electromagnetic environment, enabling the detection of healing progression through resonance frequency shifts in the antenna response.

V. CONCLUSION

This work presents an on-body slot antenna designed for real-time monitoring of cranial bone regeneration using biodegradable implants. The antenna is designed on a Rogers 3010 substrate and is enhanced with a flexible graphite-silicone composite superstrate, ensuring both partial conformity and increased in-body propagation by minimizing the near-field losses and decreasing reflections at the air to skin boundary. The simulations used a three-layer head phantom (skin, skull, and brain) with the antenna positioned above the skin and a lattice-shaped implant with a radius of 12 mm embedded in the skull, surrounded by a liquid layer to replicate post-surgical conditions. By progressively reducing the implant radius from 12 mm to 2 mm, mimicking bone regrowth and implant biodegradation, the system detected a resonance frequency shift exceeding 570 MHz. Future work will include the experimental validation of the monitoring through phantoms and animal tests.

ACKNOWLEDGMENTS

This work was supported by Bogazici University Scientific Research Fund (BAP) under project number BAP 20351 (BAP-ST 25A02P3). The authors would like to thank Trabtech for providing the biodegradable implant samples.

REFERENCES

- [1] J. Li, C. Gsaxner, A. Pepe, A. Morais, V. Alves, G. von Campe, J. Wallner, and J. Egger, "Synthetic skull bone defects for automatic patient-specific craniofacial implant design," *Scientific data*, vol. 8, no. 1, p. 36, 2021.
- [2] S. Shaikh, R. Ghosh, A. H. Pandit, S. Mehrotra, and A. Kumar, "Recent advances in biodegradable implants in bone tissue engineering," *Emerging Materials and Technologies for Bone Repair and Regeneration*, pp. 109–128, 2025.
- [3] M. Prządka, W. Pajak, J. Kleinrok, J. Pec, K. Michno, R. Karpiński, and J. Baj, "Advances in 3d printing applications for personalized orthopedic surgery: From anatomical modeling to patient-specific implants," *Journal of Clinical Medicine*, vol. 14, no. 11, p. 3989, 2025.
- [4] M. D. Perez, G. Thomas, S. R. M. Shah, J. Velander, N. B. Asan, P. Mathur, M. Nasir, D. Nowinski, D. Kurup, and R. Augustine, "Preliminary study on microwave sensor for bone healing follow-up after cranial surgery in newborns," in *12th European Conference on Antennas and Propagation (EuCAP 2018)*. IET, 2018, p. 891.
- [5] A. Mangrulkar, S. B. Rane, and V. Sunnapwar, "Automated skull damage detection from assembled skull model using computer vision and machine learning," *International Journal of Information Technology*, vol. 13, no. 5, pp. 1785–1790, 2021.
- [6] M. A. Taha, S. L. Manske, E. Kristensen, J. T. Taiani, R. Krawetz, Y. Wu, D. Ponjevic, J. R. Matyas, S. K. Boyd, D. E. Rancourt *et al.*, "Assessment of the efficacy of mri for detection of changes in bone morphology in a mouse model of bone injury," *Journal of Magnetic Resonance Imaging*, vol. 38, no. 1, pp. 231–237, 2013.
- [7] A. Saranya and K. Kottilingam, "A survey on bone fracture identification techniques using quantitative and learning based algorithms," in *2021 international conference on artificial intelligence and smart systems (ICAIS)*. IEEE, 2021, pp. 241–248.
- [8] M. Särestöniemi, D. Singh, M. von und zu Fraunberg, and T. Myllylä, "Microwave technique for linear skull fracture detection—simulation and experimental study using realistic human head models," *Biosensors*, vol. 14, no. 9, p. 434, 2024.
- [9] J. EbrahimiZadeh, M. D. Perez, and R. Augustine, "Electromagnetic time-reversal technique for monitoring skull healing stages," in *2019 13th European Conference on Antennas and Propagation (EuCAP)*. IEEE, 2019, pp. 1–5.
- [10] G. Thomas, "Extraction of follow up parameters of bone density microwave sensor from post craniotomy and lower extremity trauma rehabilitation measurements," Master's thesis, Uppsala University, 2017.
- [11] V. Mattsson, "Clinical data analysis for conceptual proof of microwave bone healing monitoring system for craniosynostosis patients," Master's thesis, Uppsala University, Uppsala, Sweden, 2018.
- [12] E. G. SanVicente, C. Henemann, J. Disser, R. Grinyte, N. Marjanović, and J. M. Cabot, "Implantable sensors and biosensors to monitor bone regeneration: Wireless smart system for on-line monitoring of ph, temperature, strain sensors and $tgf\beta 1$ during bone healing," in *2023 IEEE SENSORS*. IEEE, 2023, pp. 1–4.
- [13] K. Yu, L. Ren, Y. Tan, and J. Wang, "Wireless magnetoelasticity-based sensor for monitoring the degradation behavior of polylactic acid artificial bone in vitro," *Applied Sciences*, vol. 9, no. 4, p. 739, 2019.
- [14] A. Aldelem, E. Adjei, P. Siaw, A. Al-Dulaimi, V. Doychinov, N. T. Ali, R. Qahwaji, J. G. Buckley, P. Twigg, and R. A. Abd-Alhameed, "Monitoring bone healing: Integrating rf sensing with ai," *IEEE Access*, 2024.
- [15] M. S. Hossen, M. T. Islam, A. Hoque, A. M. Alenezi, P. Kirawanich, M. H. Baharuddin, Y. S. Faouri, and M. A. Rahman, "Revolutionizing osteoporosis and bone fracture diagnostics: The emergence of microwave antenna technology," *IEEE Access*, 2024.
- [16] D. Lee, G. Shaker, D. Nowinski, and R. Augustine, "Monitoring of healing progression of cranial vault using one-dimensional pulsed radar technique," in *2018 IEEE International Microwave Biomedical Conference (IMBioC)*. IEEE, 2018, pp. 64–66.
- [17] D. Lee, J. Velander, D. Nowinski, and R. Augustine, "A preliminary research on skull healing utilizing short pulsed radar technique on layered cranial surgery phantom models," *Progress In Electromagnetics Research C*, vol. 84, pp. 1–9, 2018.
- [18] D. Lee, D. Nowinski, and R. Augustine, "A uwb sensor based on resistively-loaded dipole antenna for skull healing on cranial surgery phantom models," *Microwave and optical technology letters*, vol. 60, no. 4, pp. 897–905, 2018.

- [19] P. Mathur, D. G. Kurup, and R. Augustine, "Design of open ended circular waveguide for non-invasive monitoring of cranial healing in pediatric craniosynostosis," in *2017 First IEEE MTT-S International Microwave Bio Conference (IMBIOC)*. IEEE, 2017, pp. 1–4.
- [20] D. Y. Kwon, J. S. Kwon, S. H. Park, J. H. Park, S. H. Jang, X. Y. Yin, J.-H. Yun, J. H. Kim, B. H. Min, J. H. Lee, W.-D. Kim, and M. S. Kim, "A computer-designed scaffold for bone regeneration within cranial defect using human dental pulp stem cells," *Scientific Reports*, vol. 5, p. 12721, 2015.